Role of surface strain in the subsurface migration of adsorbates on silicon

Juan Carlos F. Rodríguez-Reyes and Andrew V. Teplyakov*
Department of Chemistry and Biochemistry, University of Delaware, Newark, Delaware 19716, USA
(Received 29 May 2008; published 16 October 2008)

Modification of silicon surfaces through the insertion of atoms or even small molecular fragments of an adsorbate into a silicon-silicon bond can be affected tremendously by the effects of surface strain. This process takes place as either surface insertion or subsurface insertion, depending on whether the inserted species remains within the topmost layer or undergoes migration into subsurface layers, respectively. Using density-functional-theory cluster calculations, we show that insertion can be both thermodynamically and kinetically favorable if it takes place in such a way that surface strain is mitigated by neighboring surface sites. By considering the thermal decomposition of ammonia (NH_3) adsorbed on a Si(100)-2×1 surface, we find that insertion mainly depends on the initial distribution of adsorbates and the orientation taken by inserted species with respect to neighboring structures along the surface. These factors seem to greatly affect the subsurface insertion, which can therefore be considered a long-range process. On the other hand, for surface-insertion processes the factors mentioned above are less influential, and insertion has more of a local character. Understanding the factors governing insertion mechanisms may lead to development of more approaches to surface functionalization, where the adsorbates decorating the surface can decompose in a controllable fashion.

DOI: 10.1103/PhysRevB.78.165314 PACS number(s): 68.43.Bc, 68.43.Fg, 68.43.Hn, 68.47.Fg

I. INTRODUCTION

Insertion of atoms and even small fragments from adsorbate molecules into the lattice of a substrate is the basis of major industrial processes, including etching,[1,2] catalyst preparation,[3–5] and film growth.[6] In an effort to understand and control these processes, mechanisms of adsorption and decomposition on surfaces have been investigated quite extensively.[1–4,6–8] In addition, new molecular-level technologies, such as molecular electronics and surface self-assembly require new approaches to controlling the mechanisms of surface reactions, broadening the scope of surface science.[9,10]

Together with the tremendous advances made by experimental surface science, theoretical findings have played a decisive role in understanding mechanisms of surface reactions.[11–14] A combination of these approaches allowed for a controlled adsorption of organic molecules, known as surface functionalization, which constitutes the foundation of the molecular-level technologies mentioned above.[8–10] Although a myriad of adsorbates have been studied to date, there are a rather limited number of substrate materials that can be prepared and functionalized in a molecularly controlled manner. Among these substrates, silicon has been studied in great detail due to its current importance in the electronics industry.[8–10] In particular, a large number of investigations have been devoted to mechanisms of adsorption on the Si(100)-2×1 surface due to its high degree of order and its remarkable reactivity.[6–10] This silicon surface can be best described as arrays of dimer rows formed by the (2×1) reconstruction that stabilizes the surface. The stability of these dimers is further increased due to their dynamic buckling at room temperature, which confers a zwitterionic character to these surface entities.[14,15] Since silicon atoms on the surface remain unsaturated even after the (2×1) reconstruction, this surface is very reactive. For example, ammonia (NH_3) and water (H_2O) adsorb dissociatively, even at cryogenic temperatures, to form (Si)NH_2 and (Si)H moieties in the former case[16–26] and (Si)OH and (Si)H species in the latter.[27–30] Dissociated species may occupy the same dimer or neighboring dimers, known respectively as intradimer and interdimer dissociations.[26,31] Adsorption of both NH_3 and H_2O has been studied not only to functionalize a surface but also to unveil the initial stages of surface nitridation[18,19,32–36] and oxidation.[27–29,37–39] For the NH_3/Si(100) system, in particular, a previous publication extensively reviewed the literature available.[40]

In the first stage of adsorbate incorporation into a Si(100)-2×1 surface, the insertion can take place either into a Si-Si dimer bond or into a Si-Si backbond, as shown in Fig. 1 for the insertion process characteristic of (Si)NH_2 species (structure A1), obtained upon dissociative adsorption of NH_3. The sequence depicted in the left part of the figure is known as intradimer insertion or simply surface insertion and leads to structure B2. The latter case is often referred to as backbonded or subsurface insertion, producing structure S2.[40–44] In both cases, the inserting NH_3 species breaks a Si-Si bond, forming $(Si)_2NH_2$ structures (B1 and S1 for surface and subsurface insertions, respectively), where the N atom is tetracoordinated. The usual tricoordination of N is regained by transferring an H atom to the unsaturated Si surface atom, resulting in the formation of $(Si)_2NH$ structures (B2 and S2). Further decomposition is likely to take place in a similar manner: structures B3 and S3, featuring a tetracoordinated N atom, are followed by hydrogen transfer, leading to $(Si)_3N$ structures (shown as B4 and S4 in Fig. 1).

Surface insertion has often been considered more facile than subsurface insertion due to the steric effects that have to be taken into account in the latter case. Supporting this view, it has been shown that the thermal decomposition of H_2O on Si(100)-2×1 starts with the insertion of O atoms into the Si-Si dimer bond.[28] Although additional oxygen atoms can insert into the Si-Si backbond at higher temperatures, there is no evidence of oxygen migration beyond the second layer in the temperature range of 300–900 K.[27–29,37–39] On the other hand, complete decomposition of NH_3 on Si(100)-2×1

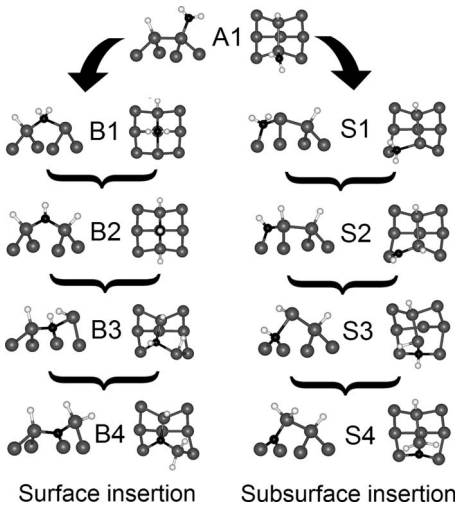

FIG. 1. Possible pathways corresponding to the thermal decomposition of NH_3 on the Si(100)-2×1 surface. Black: nitrogen; gray: silicon; white: hydrogen. Upon decomposition, structure A1 can undergo surface insertion (B1–B4) or subsurface insertion (S1–S4). For each structure, lateral and top views are included and, for clarification purposes, only silicon atoms representing the top two layers are shown in the lateral view. Surface models were simulated using the Si_9H_{12} single-dimer cluster. In all cases, hydrogen terminations of the cluster are hidden. Notice the similarities between the tetracoordinated nitrogen species (B1, B3, S1, and S3) and their immediate successors (B2, B4, S2, and S4, respectively).

results in N atoms residing between the third and fifth layers,[32–34] indicating that in this case subsurface migration is dominant. Moreover, other investigations have suggested that $(Si)NH_2$ species undergo subsurface insertion, either preferentially or competing with surface insertion.[17,32,33,40,45] Conversely, most theoretical investigations of the reaction of NH_3 with the Si(100) surface have shown that surface insertion of the nitrogen atom is preferred over subsurface insertion,[41,43] and that both processes may be unfavorable with respect to NH_3 desorption.[43] However, experimental results have shown that desorption of NH_3 is a minor channel of desorption.[16,46] This indicates that an alternative theoretical approach is needed in order to better describe insertion processes.

Theoretical investigations of surface reactions require primarily a reliable model capable of representing the surface realistically. In the case of the Si(100)-2×1 surface, the smallest model is the Si_9H_{12} cluster, representing a single surface silicon dimer.[11–13] Hydrogen atoms are used to maintain the appropriate hybridization of silicon atoms, with the logical exception of the unsaturated topmost dimer atoms. In addition to cluster calculations, slab calculations have also been used.[12,13] In this case, the basic unit is repeated *ad infinitum* using periodic boundary conditions. Since insertion mechanisms usually imply the modification of surface layers below the topmost layer, the mobility of subsurface atoms in the computational model has to be carefully considered. For this reason, atoms representing the rather stationary subsurface layers are often held at fixed positions.[11,30,40,47] Differences in predicted energies using constrained and unconstrained clusters have been previously addressed.[48–50]

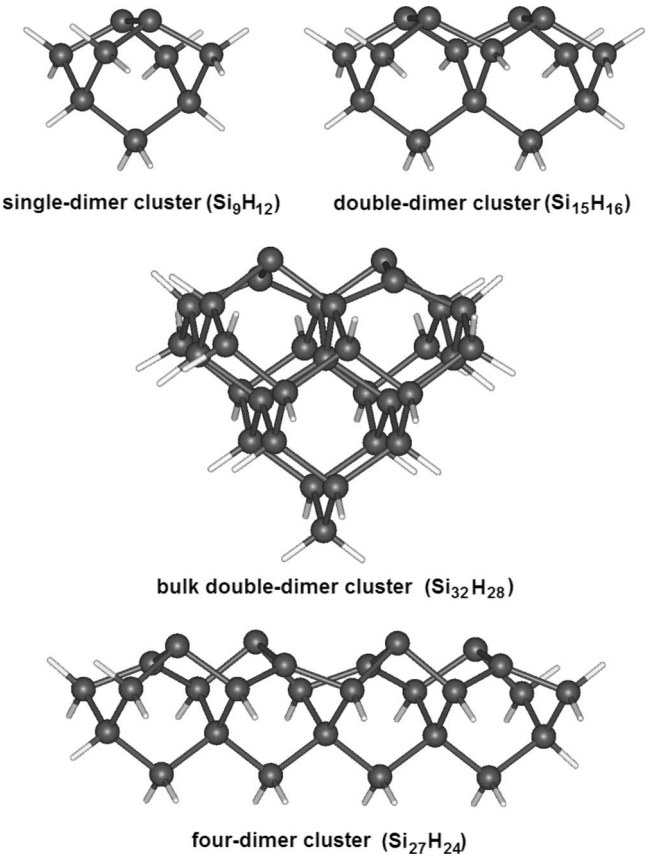

FIG. 2. Cluster models representing a Si(100) surface.

Although constrained models seem to be more realistic, they may overestimate the effects of strain on the insertion processes. In a previous publication,[40] we suggested that by considering neighboring dimers of the Si(100)-2×1 surface it may be possible to simulate mechanisms of strain relief, *even if the cluster model is constrained*. To the best of our understanding, multiple-site models of this surface have been used to investigate adsorption processes[25,26,47,51–58] but not to consider insertion mechanisms on a long-range basis. In this paper we explore the role of surface strain during insertion processes, comparing the decomposition pathways for NH_3 on Si(100)-2×1 summarized in Fig. 1.

II. COMPUTATIONAL METHODOLOGY

Density-functional-theory calculations were performed using cluster models representing one surface dimer (Si_9H_{12}) and two neighboring surface dimers along the same row ($Si_{15}H_{16}$). These models are hereafter called single-dimer and double-dimer clusters, respectively, and are shown in Fig. 2. In both cases, silicon atoms representing the top two layers of the surface and adsorbate species were allowed to relax, while the remaining atoms were held at fixed positions in order to mimic the lattice conditions. Constrained atoms were fixed after optimization of the H-saturated cluster, where the surface silicon atoms are monohydrogenated. At the level of theory employed (described below), the single- and double-dimer cluster models have predicted adsorption

energies for the $NH_3/Si(100)$ system that are very similar to those obtained using other computational models (Ref. 40, and references therein). In addition, double-dimer cluster models have been able to accurately predict vibrational frequencies of surface species.[25,40] These comparisons suggest the appropriateness of these cluster models for simulating surface reactions. However, to further validate this statement, the energy values predicted for selected structures considered in this work using these relatively small cluster models are compared to those obtained using two larger clusters, $Si_{27}H_{24}$ and $Si_{32}H_{28}$. The first of these clusters, hereafter called the four-dimer cluster model, represents four neighboring dimers along a dimer row. Constraints to subsurface atoms are applied in a similar fashion as for the single- and double-cluster models. The $Si_{32}H_{28}$ cluster, hereafter called the bulk double-dimer cluster, represents two neighboring dimers of the same row but includes a number of additional silicon atoms representing the bulk of the crystal (nine representing the third layer, six representing the fourth layer, and four representing the fifth layer). Since the intention in using this cluster was to observe the effect of subsurface insertion into the bulk, silicon atoms representing the third layer and above were allowed to relax. However, these atoms were kept at realistic positions by fixing the positions of hydrogen atoms in the termination of these layers. It will be shown that the comparison of energetic values using these models provides further support for the validity of the double-dimer cluster model used in this investigation.

Calculations were performed using the B3LYP method, which is a combination of the three-parameter exchange functional of Becke[59] with the correlation functional of Lee *et al.*[60] This method has been widely used to investigate surface reactions. Particularly for reactions on the Si(100)-2×1 surface, it has been shown that energies and geometries obtained with B3LYP are similar to other methods such as MP2[61] and QCISD(T).[62] All structures were optimized using the 6-31+$G(d)$ Gaussian basis set, which includes diffuse functions and polarization functions to the heavy atoms. Single-point energies of optimized structures were also calculated with the 6-311+$G(d,p)$ basis set, which adds polarization functions to the H atoms. In a previous publication,[40] energetic values corresponding to the formation of B2 and S2 from structure A1 (Fig. 1) using this basis set were compared to those obtained in another computational investigation[43] using the 6-311++$G(2d,p)$ basis set, which includes polarization functions and diffuse functions for all atoms. The differences in predicted energy for A1 and the first transition states (toward the formation of B1 and S1) were found to differ by approximately 5 kJ/mol, showing the sufficiency of the 6-31+$G(d)$ basis set. Transition states were calculated using the synchronous transit-guided quasi-Newton method[63] which, starting from an average geometry between initial and final structures, searches for a first-order saddle point using a quadratic-synchronous-transit approach. Predicted transition-state structures featured in all cases a single negative eigenvector, which confirms the convergence to a first-order saddle point. Calculations were performed using the GAUSSIAN03 suite of programs.[64]

TABLE I. Predicted energies (kJ/mol) for structures proposed for the surface and subsurface insertions of nitrogen during decomposition of NH_3 on Si(100)-2×1. Single-point energies at the B3LYP/6-311+$G(d,p)$ level of theory were calculated upon optimization at the B3LYP/6-31+$G(d)$ level of theory. Constrained and unconstrained Si_9H_{12} single-dimer clusters are used to represent the surface, together with constrained $Si_{15}H_{16}$ double-dimer clusters. When insertion can take place in two orientations for the double-dimer cluster model (inward or outward), both energies are reported. In all cases, the values are given with respect to the empty cluster model and NH_3.

Surface-insertion pathway	Single dimer, unconstrained	Single dimer, constrained	Double dimer, constrained
A1	−213.6	−221.0	−233.9
B1	−124.2	−125.1	−150.8
B2	−255.2	−253.5	−262.5
B3	−101.9	−24.0	−28.2/−38.9
B4	−261.9	−198.5	−172.4/−199.0

Subsurface-insertion pathway	Single dimer, unconstrained	Single dimer, constrained	Double dimer, constrained
A1	−213.6	−221.0	−233.9
S1	−119.9	−112.8	−98.5/−131.3
S2	−250.8	−243.9	−213.6/−251.6
S3	−130.9	−106.2	−101.4
S4	−287.6	−275.4	−253.1

III. RESULTS

A. Constrained versus unconstrained cluster models: Simulation of surface strain

As indicated above, a correct simulation of a surface by a cluster model requires the use of geometrical constraints for atoms representing subsurface layers. Table I compares the stability of the surface structures described in Fig. 1, using constrained and unconstrained single-dimer cluster models. Based on these values, it can be concluded that the use of constraints does not affect significantly the stability of structures involving minor changes in the position of the atoms representing the subsurface layers (e.g., structures A1, B1, and B2). Differences between constrained and unconstrained models become pronounced when the lattice is modified substantially by the insertion process, as can be observed for structures undergoing subsurface insertion (S1–S4), but more drastically for structures B3 and B4. In these cases, the use of unconstrained clusters leads to a significant increase in the predicted stability because the strain imposed can be easily redistributed by altering the position of the atoms representing the third and lower layers.

Despite the advantages of constrained single-dimer cluster models, there are some uncertainties that become apparent as the specifics of the insertion mechanisms are considered. In these models, the movement of the atoms representing the third and lower layers is completely restricted,[11,30,40,47] thus making it nearly impossible for the overall structure to adjust

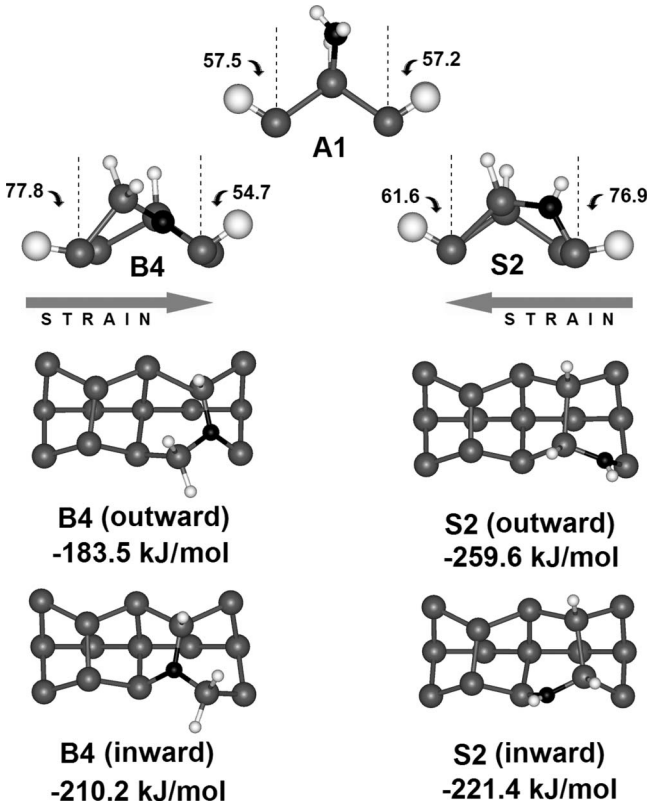

FIG. 3. Effect of insertion on the mobile H_{term} entities of the cluster model representing the surface. Gray: silicon; black: nitrogen; small white: hydrogen; large white: H_{term} entities. For structures A1, B4, and S2 simulated using a single-dimer cluster model, the angles of these entities with respect to the surface normal are shown. Large arrows for structures B4 and S2 indicate the direction of strain, which opposes the most dramatic displacement of atoms on the surface. The replacement of H_{term} entities by a neighboring dimer results in two possibilities of insertion, indicated as inward and outward. The stability of a structure varies depending on whether or not strain can be simulated by a neighboring dimer. Geometries were optimized at the B3LYP/6-31+$G(d)$ level of theory. Energies shown correspond to single-point calculations at the B3LYP/6-311+$G(d,p)$ level of theory. For clarification purposes, only silicon atoms representing the top two layers are shown for the single-dimer cluster models.

and compensate for the strain effects during the insertion process. Atoms representing the two topmost layers are unconstrained, but their mobility is very much limited by the fixed positions of the surrounding atoms. On the other hand, hydrogen atoms emulating the positions of topmost silicon atoms surrounding the dimer under investigation are often not constrained. For example, in the Si_9H_{12} cluster there are H atoms simulating the two neighboring silicon dimers along the same dimer row, as shown in Fig. 3 for structure A1. These hydrogen atoms, hereafter called H_{term} atoms, are allowed to move rather easily upon any structural change. However, in several cases the positions of H_{term} atoms remain essentially unchanged. For example, at the B3LYP/6-31+$G(d)$ level of theory, the angles between H_{term} entities in the Si_9H_{12} cluster model and the surface normal are 57.5° and 57.2° for structure A1, which is very close to the predicted angle of 56.3° for an unoccupied single-dimer cluster model. This indicates that the positions of H_{term} entities in structure A1 emulate the positions of neighboring dimers quite well. In contrast, simulation of other structures may result in substantial repositioning of H_{term} entities. Figure 3 exemplifies this statement by analyzing this phenomenon in structures B4 and S2. Although it is not shown, similar changes take place in structures B3 and S1; for structures B1 and B2 and S3 and S4, the positional change is less noticeable. Analysis of the same angle for structures B4 and S2 shows that in both cases there is one H_{term} atom that changes its position significantly (77.8° and 76.9°, respectively), while the other features a less significant change (angles of 54.7° and 61.6°, respectively). These H_{term} entities change their positions because they cannot oppose the structural changes produced upon insertion or, in other words, they cannot simulate the effect of surface strain. Thus, the fact that one H_{term} is affected more than the other suggests that surface strain rises laterally, opposing the displacement of atoms on the surface. Further discussion of the effects of surface strain will be mostly focused on structures S2 and B4 because they exhibit the largest deviation of the H_{term} atoms from their original positions. Figure 3 shows the general direction of surface strain as insertion leads to these structures. For structure S2 such force is basically opposed to the path of nitrogen insertion. For structure B4, it parallels the direction of nitrogen insertion.

Since the movement of easily displaceable H_{term} entities indicates the points where most of the surface strain is generated, the inclusion of a neighboring dimer replacing these entities should result in a more reliable model that would resemble the structure of a continuous surface more closely. This is shown in Fig. 3, where double-dimer cluster models are used to describe structures B4 and S2. Two possibilities for the insertion process are shown, depending on whether nitrogen insertion occurs inward or outward with respect to the C_2 rotational axis of an unoccupied double-dimer cluster. (These directions of insertion will be hereafter called *inward* and *outward*, respectively.) Formation of structures S2 (outward) and B4 (inward) features stabilities similar to those obtained using a single-dimer cluster because insertion is to be opposed by H_{term} entities, which instead of simulating strain effects are allowed to reposition themselves within these models. Structures S2 (inward) and B4 (outward), on the other hand, feature a decreased stability compared to that obtained using the single-cluster model because in these cases the effect of surface strain is simulated by the neighboring dimer.

Table I shows the energies predicted for structures involved in both decomposition pathways, using a double-dimer cluster. Similar to the already discussed structures B4 and S2, their respective predecessors B3 and S1 also have two possibilities for insertion and their stability decreases (with respect to the single-dimer cluster model) when a neighboring dimer can simulate strain effects. Other structures, such as S3 and S4, also show a decreased stability in the double-dimer model with respect to that obtained from a single-dimer cluster, indicating that these structures do impose certain strain on the lattice. However, in this case the decrease in stability may be attributed to the formation of

two Si-N bonds (relatively short compared to Si-Si bonds) with subsurface atoms, which affects the second layer. The increase in stability for structures where the double-dimer model is used instead of the single-dimer model (e.g., A1, B1, and B2) can be attributed to the more efficient redistribution of electronic density from the N atom to the cluster as its size increases.[47]

Thus, it has been shown that the amount of strain imposed upon insertion, as well as its direction, varies depending on the model structures considered. Therefore, pathways of insertion are better represented not only by constrained clusters but also by representing the neighboring surface units that can be affected by this surface modification. Section III B will discuss the nature of the strain imposed on the lattice when the insertion process occurs on neighboring surface dimers.

B. Insertion as a long-range process: Mitigation of surface strain

A surface saturated by ammonia is a more practical model than a single ammonia molecule on a silicon surface, as most experiments and practical applications use high ammonia coverages. This case can be represented by a double-dimer cluster where each dimer features $(Si)NH_2$ and (Si)H species (two of structures A1 together, which is hereafter described using the notation A1-A1). These two structures can exist in several different distributions along a dimer row, as we discussed in a previous publication.[40] Briefly, it is possible that the $(Si)NH_2$ species are located on different sides along a dimer row (alternate distribution, Fig. 4) or on the same side along a row (aligned distribution, Fig. 5). A less likely distribution, which we have called agglomerate distribution, occurs when one dimer holds two $(Si)NH_2$ species and the neighboring dimer accommodates two (Si)H species. Since it has been observed that alternate and aligned distributions are dominant on the surface,[25,40,53–56,65,66] we will focus on these two configurations and will not consider any agglomerate distributions further for the purposes of this discussion.

Alternate structure A1-A1 can undergo the same decomposition pathway as shown in Fig. 1 but, similar to the case observed above for the double-dimer cluster model, inserted structures may be directed either inward or outward. Structures following the decomposition of A1-A1 were optimized (considering all possible orientations of structures) and the energies obtained are tabulated in Table II. Figure 4 shows the most relevant structures in the course of insertion. From Table II, it is possible to see that structures B1-B1 and B2-B2 do not exhibit any significant difference in their stability when compared to the values obtained from a single-dimer cluster model (B1 and B2, Table I). This indicates that in this case the strain imposed is simulated rather well even by a single-dimer cluster, which is expected since this structure does not affect significantly the positions of the subsurface atoms. In contrast, structures S3-S3 and S4-S4 decrease their predicted stability with respect to the single-adsorbate models, showing that a cluster larger than a single-dimer might represent better the strain produced by the formation of subsurface $(Si)_3N$ species.

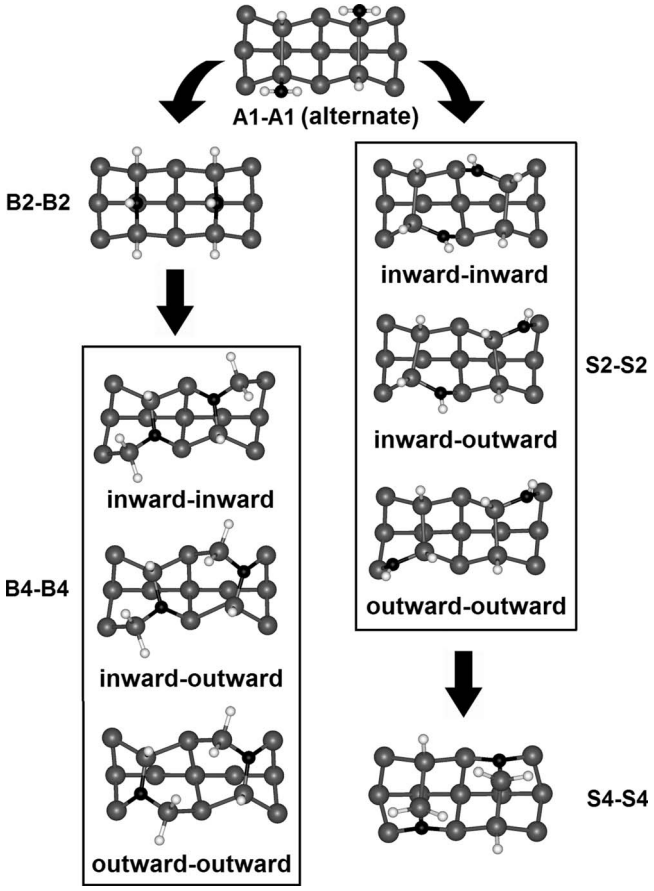

FIG. 4. Pathways of decomposition for an alternate structure A1-A1. Gray: silicon; black: nitrogen; white: hydrogen. The surface is represented by a $Si_{15}H_{16}$ double-dimer cluster model. Top views are shown for all structures, with H terminations of the cluster model hidden to facilitate visualization. For simplification purposes, tetracoordinated N structures B1, B3, S1, and S3 are not shown (those are similar to B2, B4, S2, and S4, respectively). Structures B4 and S2 feature three different orientations. Geometries were optimized at the B3LYP/6-31+$G(d)$ level of theory.

A more interesting type of variation occurs when the stability of decomposed structures depends on the orientation of nitrogen insertion with respect to the same process on the neighboring dimer. This is observed for structures B3-B3, B4-B4, S1-S1, and S2-S2, where inward-inward, inward-outward, and outward-outward configurations are all possible (Fig. 4). It was shown in Fig. 3 that structures B4 (inward) and S2 (outward) produce relatively stable structures because H_{term} entities cannot simulate surface strain. Similarly, Table II shows that the inward-inward orientation for structures B3-B3 and B4-B4 and the outward-outward orientation for structures S1-S1 and S2-S2 feature higher stabilities compared to other orientations. However, if the only manner of increasing the predicted stability were through the repositioning of H_{term} entities, it would be expected that the inward-outward orientation produces structures with stabilities lying between those of inward-inward and outward-outward orientations, which is not the case. For example, structure B4-B4 (outward-outward) is found to be more stable than structure B4-B4 (inward-outward). Thus, strain

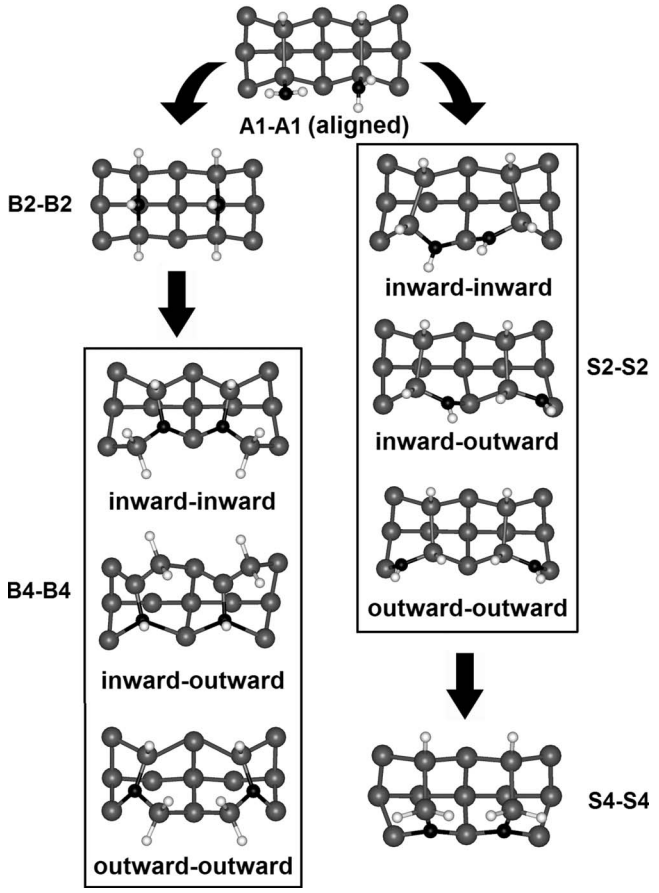

FIG. 5. Pathways of decomposition for an aligned structure A1-A1. Gray: silicon; black: nitrogen; white: hydrogen. The surface is represented by a $Si_{15}H_{16}$ double-dimer cluster model. Top views are shown for all structures, with H terminations of the cluster model hidden to facilitate visualization. For simplification purposes, tetracoordinated N structures B1, B3, S1, and S3 are not shown (those are similar to B2, B4, S2, and S4, respectively). Structures B4 and S2 feature three different orientations. Geometries were optimized at the B3LYP/6-31+$G(d)$ level of theory.

effects are maximized when the inward-outward orientation is used and may be minimized for outward-outward orientations. Figure 4 shows that structure B4-B4 (inward-outward) indeed distorts the lattice substantially, which explains its lower stability compared to other arrangements. This figure shows also a significant level of distortion for structure S2-S2 (inward-outward) with respect to the same structure in other orientations. However, in this case structure S2-S2 (inward-outward) is slightly more stable than S2-S2 (inward-inward).

In the case of inward-inward and outward-outward orientations (for both B4-B4 and S2-S2), the strain generated by the insertion process initiated on one surface dimer is partially compensated for by the strain imposed by the insertion process on a neighboring dimer, resulting in the mitigation of the strain. Oppositely, strain from two neighboring dimers in the inward-outward orientation has the same direction and no counteracting effects can be observed. Since the orientation of two neighboring structures can affect the rise of strain effects and therefore the stability of surface products, it may be expected that insertion pathways that alleviate the strain of the insertion process most efficiently will prevail in dictating the long-range dependencies of the insertion sequences. Thus, our calculations suggest that the *orientation* of structures produced *during* decomposition has a profound effect on the *strain compensation* and, therefore, on the *occurrence of a specific decomposition pathway*.

Decomposition pathways of aligned structures are shown in Fig. 5 and their corresponding energies are displayed in Table II. In this case, inward-inward orientations for structures S1-S1 and S2-S2 and outward-outward ones for structures B3-B3 and B4-B4 feature a lower stability than in the alternate distribution. This is due to the fact that inserting structures are on the same side of the dimer row and steric effects play a more significant role. Aligned structure B3-B3 (inward-inward) was in fact so unstable that in the course of optimization it converged to other structures; for this reason it is shown as n/a in Table II. Nevertheless, our previous observations are confirmed by this set of calculations: inward-outward orientations increase the straining effects due to the substantial distortion of the lattice, resulting in a lower stability than in other orientations [particularly, with respect to orientations such as S2-S2 (outward-outward) and B4-B4 (inward-inward), where neighboring dimers cannot simulate surface strain effects].

It is worth noticing that the stability of some inserted structures depends on the initial distribution of surface species. Table II shows that aligned structure S4-S4, for example, is approximately 40 kJ/mol less stable than the same structure in the alternate pattern. The same trend is observed for structure B1-B1. This suggestion will be further analyzed in Sec. IV.

C. Sequential versus coordinated models of insertion: Feasibility of decomposition pathways

So far, it has been demonstrated that the orientation of inserted species plays a fundamental role in the stability of inserted structures. The calculation of potential-energy diagrams (PEDs) requires the design of a detailed pathway for insertion that would become a long, tedious task if all structures, distributions, and orientations discussed above were considered. Previous theoretical investigations have shown that the formation of $(Si)_2NH$ structures (either B2 or S2) is the critical step during insertion.[42] For this reason, this section will be limited to the analysis of the steps A1→B1→B2 and A1→S1→S2.

The kinetics of the formation of B2 and S2 will be investigated first considering a model in which the $(Si)NH_2$ structure (A1) has a neighboring dimer featuring an inserted structure $(Si)_2NH$ (either the surface structure B2 or the subsurface structure S2). These possibilities are shown in Fig. 6. Following the notation presented in this figure, the surface pathway is represented by

$$\mathbf{A1}\text{-B2} \rightarrow \mathbf{B1}\text{-B2} \rightarrow \mathbf{B2}\text{-B2}. \quad (1)$$

Similarly, the subsurface-insertion pathway is represented by

$$\mathbf{A1}\text{-S2} \rightarrow \mathbf{S1}\text{-S2} \rightarrow \mathbf{S2}\text{-S2}. \quad (2)$$

TABLE II. Predicted energies (kJ/mol) for structures proposed for the surface and subsurface insertions of nitrogen during decomposition of NH_3 on Si(100)-2×1. Single-point energies at the B3LYP/6-311 $+G(d,p)$ level of theory were calculated upon optimization at the B3LYP/6-31$+G(d)$ level of theory. A saturated surface is represented by a constrained $Si_{15}H_{16}$ double-dimer cluster with two NH_3 molecules. Alternate and aligned distributions of adsorbates are considered, together with all possible orientations of inserted structures. In all cases, the values are given with respect to the empty double-dimer cluster and two NH_3 molecules.

Surface-insertion pathway	Alternate (in-in)	Alternate (in-out)[a]	Alternate (out-out)[a]	Aligned (in-in)[a]	Aligned (in-out)[a]	Aligned (in-out)[a]
A1-A1	−226.9			−228.9		
B1-B1	−134.2			−117.4		
B2-B2	−255.9			−255.9		
B3-B3	−20.8	−6.9	−25.3	−15.3	−20.5	n/a[b]
B4-B4	−189.9	−163.1	−180.6	−199.5	−184.1	−130.0
Subsurface-insertion pathway	**Alternate (in-in)**	**Alternate (in-out)[a]**	**Alternate (out-out)[a]**	**Aligned (in-in)[a]**	**Aligned (in-out)[a]**	**Aligned (out-out)[a]**
A1-A1	−226.9			−228.9		
S1-S1	−91.2	−94.2	−116.4	−52.5	−98.2	−107.4
S2-S2	−215.9	−225.1	−247.2	−203.8	−225.4	−245.1
S3-S3	−85.8			−52.7		
S4-S4	−247.7			−209.0		

[a]Structures A1-A1, B1-B1, B2-B2, S3-S3, and S4-S4 feature only one possible orientation for each distribution using the double-dimer cluster model.

[b]Not applicable; structure was thermodynamically unfavorable and converged to other structures.

Notice that only one of the adsorbates (in bold) undergoes insertion. Since this model corresponds to the insertion that follows the insertion process completed on the neighboring dimer, it will be referred to as the *sequential model of insertion*. Potential-energy diagrams for the sequential model of insertion were calculated and the results are presented in Table III, together with the values corresponding to the same insertion processes on a single-dimer cluster model.

Kinetics of insertion can be approached either by considering the kinetic barriers for each transformation (denoted as E_b in Table III) or by finding the overall barrier for the insertion process under investigation, which is defined as the difference between the initial state and the highest point along the energy landscape. (For the processes under investigation, it is the difference between the A1-A1 structure and the second transition state leading to S2-S2 or B2-B2.) Since individual kinetic barriers for surface insertion are greater than the ones corresponding to subsurface insertion, it may be straightforwardly assumed that surface insertion is more hindered kinetically on the surface. However, due to the fact that insertion is a two-step process where the stability of the $(Si)_2NH_2$ intermediate (B1 or S1) influences the kinetic landscape, the overall barrier for the formation of $(Si)_2NH$ structures seems to better represent the transformations under consideration.

The surface-insertion pathway has only one possibility because once the highly symmetric bridge structure B2 is formed on one dimer, the same overall configuration is obtained regardless of the initial distribution of adsorbates. Using the sequential model of insertion for the formation of the

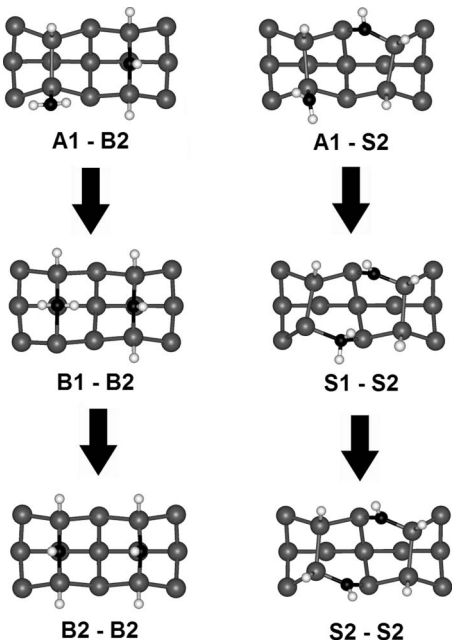

FIG. 6. Sequential model of insertion for an alternate distribution of adsorbates. The insertion process is simulated to take place once the neighboring dimer features an $(Si)_2NH$ inserted structure (B2 or S2 for surface or subsurface insertion, respectively). Gray: silicon; black: nitrogen; white: hydrogen. Although for subsurface insertion there are three possible structures, as shown in Fig. 4, only the one corresponding to the inward-inward orientation is displayed for clarification purposes. All the possibilities for both alternate and aligned distributions are discussed in the text.

TABLE III. Energy values (kJ/mol) predicted for the potential-energy diagram of formation of $(Si)_2NH$ structures following the sequential model of insertion. Transition states (TSs), individual kinetic barriers (E_b), and the overall barrier for the transformation under investigation are shown. Single-point energies at the B3LYP/6-311+$G(d,p)$ level of theory were calculated upon optimization at the B3LYP/6-31+$G(d)$ level of theory. In all cases, the values are given with respect to NH_3 and the double-cluster model with one $(Si)_2NH$ structure. For comparison, values corresponding to the potential-energy diagram using a single-dimer cluster model are included.

Surface-insertion pathway	Alternate (in-in)	Alternate (out-out)[a]	Alternate (in-out)[a]	Aligned (out-out)[a]	Aligned (in-out)[a]	Aligned (out-out)[a]	Single dimer
A1-B2	−221.1						−221.0
TS 1	22.7						27.2
(E_b)	(243.8)						(248.2)
B1-B2	−129.3						−125.1
TS 2	32.1						28.9
(E_b)	(161.4)						(154.0)
B2-B2	−249.3						−253.5
Overall barrier	253.2						249.8

Subsurface-insertion pathway	Alternate (in-in)	Alternate (in-out)	Alternate (out-out)	Aligned (in-in)	Aligned (in-out)	Aligned (out-out)	Single dimer
A1-S2	−219.5	−222.9	−222.9	223.3	−222.0	−222.0	−221.0
TS 1	11.5	4.6	8.8	−2.6	7.9	8.7	−3.5
(E_b)	(231.0)	(227.5)	(231.7)	(223.3)	(229.9)	(230.6)	(217.5)
S1-S2	−87.9	−67.6	−113.5	−66.5	−65.0	−104.3	−112.8
TS 2	60.9	91.0	−24.3	78.9	91.0	16.7	50.3
(E_b)	(148.8)	(158.6)	(89.2)	(145.5)	(156.0)	(120.9)	(163.1)
S2-S2	−218.3	−198.6	−242.9	−194.0	−199.2	−238.7	−243.9
Overall barrier	280.4	313.9	198.6	304.9	313.0	238.6	271.3

[a]There is no difference in distributions and/or orientations for this pathway.

$(Si)_2NH$ structure B2, an overall barrier very similar to the one obtained using the single-dimer cluster is obtained, showing that the presence of a neighboring dimer does not affect significantly the kinetics of insertion in this case.

The subsurface-insertion pathway shows substantial differences in the kinetics depending on the initial distribution of adsorbed A1-A1 structures and on the orientation of inserted species leading to structure S2-S2. For the alternate configuration, large disparities are found not only compared to the single-dimer cluster but also among different orientations. The outward-outward orientation is observed to be more thermodynamically favored than the inward-inward and inward-outward orientations, although it is likely that it is caused by the inability of H_{term} entities to simulate strain effects. For this reason, a better comparison can be made between the inward-inward and the inward-outward orientations. In both cases, the potential-energy diagram corresponds to an inward insertion. But in one case the neighboring unit has undergone an inward insertion and in the other it was a subject of an outward insertion.

Insertion resulting in S2-S2 (inward-inward) produces a final structure whose stability is similar to that of the starting structure A1-S2 and which is more stable than S2-S2 (inward-outward). This further supports the idea that subsurface-insertion processes may not be thermodynamically unfavorable if the strain can be alleviated through the proper combination of orientations of adsorbates on neighboring surface units. The comparison of the overall barriers for formation of S2-S2 shows that the orientation affects not only the thermodynamics of insertion but also the kinetics of these processes. The overall barrier corresponding to the inward-inward orientation of S2-S2 is not only smaller than for the inward-outward orientation but also close to the one obtained using the single-dimer cluster. The most striking difference, however, is observed for the formation of S2-S2 (outward-outward), where a very small kinetic barrier for the transformation S1-S2 → S2-S2 lowers the overall barrier significantly. It may be argued that such a barrier is obtained due to the inability of H_{term} atoms to oppose the insertion. However, this barrier is significantly lower than the one obtained using the single-dimer cluster model, where H_{term} entities surround the dimer undergoing insertion and do not simulate strain effects. Nevertheless, the comparison of insertion in the three orientations suggests that the *orientation of neighboring inserted structures* has a *profound effect* on the *energy landscape* of the subsurface-insertion process.

Similar conclusions can be drawn by analyzing the kinetics of insertion for the aligned distribution (Table III), although insertion seems to be less advantageous than when the initial distribution is alternate. Particularly, the inward-

TABLE IV. Energy barriers (kJ/mol) predicted for the potential-energy diagram of formation of $(Si)_2NH$ structures starting with the alternate configuration and following the coordinated model of insertion. Single-point energies at the B3LYP/6-311+$G(d,p)$ level of theory were calculated upon optimization at the B3LYP/6-31+$G(d)$ level of theory. For comparison, values corresponding to the potential-energy diagram using a single-dimer cluster model are included.

Surface-insertion pathway	In-in orientation	In-out orientation[a]	Out-out orientation[a]	Single dimer
	242.9			
A1-A1 → B1-B1	254.8			248.2
	170.0			
B1-B1 → B2-B2	161.4			154.0
Subsurface-insertion pathway	**In-in orientation**	**In-out orientation**	**Out-out orientation**	**Single dimer**
A1-A1 → S1-S1	222.8	231.5	231.5	
	229.7	222.8	233.0	217.5
S1-S1 → S2-S2	163.8	160.3	166.5	
	148.8	158.6	89.2	163.1

[a]There is no difference in orientation for this pathway.

inward orientation features an increased overall barrier with respect to the alternate case, due to the steric effects present during insertion of aligned structures. Similar to what was observed for the alternate distribution, formation of an S2-S2 (outward-outward) structure features an overall barrier smaller than that obtained from the single-dimer cluster model, and the overall barrier for the inward-outward orientation is found to be the most demanding.

In addition to the sequential models described in Eqs. (1) and (2), it is possible to investigate the first stages of insertion assuming a step-by-step process, starting from structure A1-A1. Following the notation used in those equations, a starting structure A1-A1 would be transformed according to

$$\text{A1-A1} \rightarrow \text{A1-B1} \rightarrow \text{B1-B1} \rightarrow \text{B2-B1} \rightarrow \text{B2-B2} \quad (3)$$

and

$$\text{A1-A1} \rightarrow \text{A1-S1} \rightarrow \text{S1-S1} \rightarrow \text{S2-S1} \rightarrow \text{S2-S2}, \quad (4)$$

for surface and subsurface insertions, respectively. Since both adsorbates undergo the insertion in a step-by-step fashion, this model will be hereafter called *coordinated model of insertion*. In order to limit the extent of the investigation of this model of insertion, only the alternate configuration is considered as a starting structure. Notice that in this model the formation of tetracoordinated intermediates (B1-B1 or S1-S1) involves the calculation of two energy barriers. The formation of $(Si)_2NH$ species (B2-B2 or S2-S2) requires the calculation of two energy barriers as well. These individual kinetic barriers are shown in Table IV and, for comparison, kinetic barriers corresponding to the same insertion processes using the single-dimer cluster models are included. The analysis of the barriers corresponding to the formation of structures B1-B1 and S1-S1 shows that the first barrier of insertion is lower than the second one. Transformation to B2-B2 and S2-S2 requires two additional barriers, and it is found that in this case the first barriers are more demanding than the second ones. Equations (3) and (4) show that the barriers that are found to be more demanding correspond to transformations involving the presence of either S1 or B1 as starting structure (e.g., A1-B1 → B1-B1 or S1-S1 → S1-S2). Thus, the differences in the pairs of energy barriers suggest that insertion is more difficult when a neighboring dimer features a tetracoordinated N structure. This is explained by the fact that Si-N bonds are longer when N is tetracoordinated than when it is in its regular tricoordination. Longer bonds imply a major displacement of Si atoms in the lattice and therefore induce more strain that affects the insertion in the neighboring dimer. By analyzing only one portion of the coordinated model of insertion, corresponding to

$$\text{A1-B1} \rightarrow \text{B1-B1} \rightarrow \text{B2-B1}, \quad (5)$$

$$\text{A1-S1} \rightarrow \text{S1-S1} \rightarrow \text{S2-S1}, \quad (6)$$

it is possible to gain more insights into the effect of the presence of tetracoordinated N structures in the neighboring dimer. In addition, the consideration of these pathways, "carved" from the coordinated model of insertion, allows the calculation of an insertion barrier, making the comparison with the sequential model more effective.

Table V summarizes the potential-energy diagrams corresponding to Eqs. (5) and (6). In all cases, insertion barriers are greater than those obtained from the sequential model of insertion (Table III). In the case of surface insertion the variation is rather small; but for subsurface-insertion barriers there is a more considerable difference, particularly for inward-inward and outward-outward orientations. In addition, stabilities of all structures are lower than those found in the sequential model of insertion, indicating that the presence of a structure bearing a tetracoordinated N atom affects the stability of inserted structures in the neighboring dimer. Thus, since our calculations show that the presence of tetracoordinated N structures affects negatively the thermodynamics and the kinetics of insertion processes, it can be deduced that such processes are more favored if they occur sequentially rather than in a coordinative fashion.

D. Double-dimer versus larger cluster models: Accuracy and uncertainties of the present results

As discussed above, using cluster models for understanding subsurface migration may lead to possible underestimation of strain because of the use of the mobile H_{term} atoms. For example, the comparison of stability for structures S2-S2 (inward-inward) and S2-S2 (inward-outward) in the alternate configuration showed that the latter orientation is more stable than the former (Table II). However, the greater stability of the inward-outward orientation was attributed to the underestimation of strain effects due to the ability of H_{term} entities to dissipate the strain (which does not happen in the inward-inward orientation). This suggestion was retested simulating these two models using a four-dimer cluster, where H_{term}

TABLE V. Energy values (kJ/mol) predicted for the potential-energy diagram of formation of $(Si)_2NH$ structures following the coordinated model of insertion. TSs, individual kinetic barriers (E_b), and the overall barrier for the transformation under investigation are shown. Single-point energies at the B3LYP/6-311 $+G(d,p)$ level of theory were calculated upon optimization at the B3LYP/6-31$+G(d)$ level of theory. In all cases, the values are given with respect to NH_3 and the double-cluster model with one $(Si)_2NH_2$ structure. For comparison, values corresponding to the potential-energy diagram using a single-dimer cluster model are included.

Surface-insertion pathway	Alternate (in-in)	Alternate (out-out)[a]	Alternate (in-out)[a]	Single dimer
A1-B1	−202.4			−221.0
TS 1	52.3			27.2
(E_b)	(254.8)			(248.2)
B1-B1	−117.6			−125.1
TS 2	52.4			28.9
(E_b)	(170.0)			(154.0)
B2-B1	−241.0			−253.5
Insertion barrier	254.9			249.8

Subsurface-insertion pathway	Alternate (in-in)	Alternate (in-out)	Alternate (out-out)	Single dimer
A1-S1	−207.9	−213.5	−213.5	−221.0
TS 1	21.8	9.3	19.5	−3.5
(E_b)	(229.7)	(222.8)	(233.0)	(217.5)
S1-S1	−83.9	−57.1	−101.4	−112.8
TS 2	80.0	103.2	65.1	50.3
(E_b)	(163.8)	(160.3)	(166.5)	(163.1)
S2-S1	−203.0	−187.8	−233.7	−243.9
Insertion barrier	287.9	316.8	278.6	271.3

[a]There is no difference in orientation for this pathway.

atoms of the two central dimers undergoing insertion are replaced by fully described silicon dimers. In this case, the stability of structure S2-S2 (inward-outward) is predicted to be −208.1 kJ/mol, which is 17.0 kJ/mol less stable than what was predicted using the double-dimer cluster (Table II). On the other hand, the stability of structure S2-S2 (inward-inward) in this large cluster is predicted to be −215.4 kJ/mol, only 0.5 kJ/mol different from the results using the double-dimer model (Table II). Thus, as speculated above, insertion mechanisms can be simulated quite reliably with small cluster models as long as the processes considered do not involve very substantial reorientation of H-terminating atoms of the cluster model. For this reason, the stabilities of structures such as A1 and the bridging structure B2 do not change considerably upon changing the size of the cluster model, as it was shown above.

The effect of the bulk, including a better representation of the subsurface layers by the cluster model, was investigated using the bulk double-dimer ($Si_{32}H_{28}$) cluster. In this case, the predicted stability for alternate structures S2-S2 (inward-inward) and S2-S2 (inward-outward) was −214.9 and −219.3 kJ/mol, respectively. By comparing these values to those shown in Table II for the double-dimer cluster model, it is obvious that the differences in stability are basically unaffected by the inclusion of more subsurface atoms. In particular, the difference for the structures S2-S2 (inward-inward) is found to be only 1.0 kJ/mol, further supporting the sufficiency of the double-dimer cluster for investigating insertion processes.

IV. DISCUSSION

The present investigation has considered cluster models with the same methods for constraining the cluster (when applicable) and the same level of theory. These similarities allow us to present a more detailed discussion regarding the nature of insertion mechanisms, which is done in Secs. IV A and IV B, focusing on the impact of surface strain and the factors governing its rise or mitigation. Section IV C includes a discussion regarding the validity of the model employed, while Sec. IV D briefly covers the consequences of our findings for practical applications.

A. Impact of surface strain on insertion processes

For structures that do not involve a significant modification of the lattice, the use of constraints is not capital in predicting the stability of surface structures, as can be seen in Table I for structures A1, B1, and B2. In the latter two cases, surface insertion takes place by breaking a Si-Si dimer bond and results in the displacement of dimer atoms, without a significant displacement of atoms in the subsurface layers. Thus, formation of B2 can be considered a "localized" process. Tables III and IV show only a slight difference in the energy landscape of surface insertion, offering further support for the local character of this process. In contrast, other insertion mechanisms (e.g., formation of structures S2 and B4) are more characteristic of a "long-range" process because the strain rises from a neighboring dimer, depending on the direction of insertion, as shown in Fig. 3.

Additional insight into the effects of strain on the stability of an inserted structure can be obtained from the comparison of the predicted stability using constrained and unconstrained models, as exemplified for the formation of structure S2 in Table VI. Unconstrained cluster calculations describe the stability gained upon formation of S2 without an effective simulation of surface strain. The difference between this stability gain and the stability gained (or lost) when a more realistic model is used can be viewed as a coarse measure of the stability loss due to the rise of surface strain. Table VI shows that using a constrained single-dimer cluster surface strain upon formation of S2 accounts for a stability loss (E_{strain}) of 14.3 kJ/mol. When a neighboring dimer opposed to the direction of insertion is included, the E_{strain} increases to 57.3 kJ/mol. Straining effects following the sequential model of insertion are maximized for the formation of alternate structure S2-S2 (inward-outward) and aligned structure S2-S2 (inward-inward). Since the loss of stability due to surface strain is larger than the stability gained in absence of strain, formation of structure S2 would be expected to be significantly unfavorable thermodynamically.[41,43] However,

TABLE VI. Stability of structure S2 with respect to A1, $\Delta E_{(S2\text{-}A1)}$, using several different models. The comparison of $\Delta E_{(S2\text{-}A1)}$ for any constrained model to the value obtained from the unconstrained cluster model offers an approximate measure of the stability loss due to the simulation of surface strain (E_{strain}). Values are reported in kJ/mol and are obtained from single-point calculations at the B3LYP/6-311+$G(d,p)$ level of theory of optimized structures at the B3LYP/6-31+$G(d)$ level of theory.

Insertion model	$\Delta E_{(S2\text{-}A1)}$	E_{strain}
Single dimer, unconstrained	−37.2	0.0
Single dimer, constrained	−22.9	14.3
Unsaturated model, double dimer	20.3	57.5
Sequential model, double dimer (alternate, in-out)	24.3	61.5
Sequential model, double dimer (aligned, in-in)	29.3	66.5
Sequential model, double dimer (alternate, in-in)	1.2	37.4

for the alternate structure S2-S2 (inward-inward) straining effects are reduced at least by 20 kJ/mol with respect to the other models using the double-dimer cluster model. This mitigation of strain effects is characteristic of the orientation that is considered. Interestingly, the comparison of E_{strain} for this arrangement to the value obtained for the double-dimer cluster with structure S2 (inward) suggests that saturation is a requisite toward the relief of surface strain. Moreover, since E_{strain} is calculated per NH_3 molecule (i.e., per dimer), an approximation of the insertion stress can be calculated by considering the surface area involved in the transformation. This possibility is, however, beyond the aim of the present investigation and will not be explored here. Nevertheless, this simple approach allows the realization that subsurface insertion cannot be assumed to be an isolated process.

B. Factors governing the rise and relief of surface strain

1. Initial distribution of adsorbates

Although the differences in stabilities of chemisorbed species A1 in the aligned and alternate distributions are not substantial (Table II), the thermodynamic course of insertion depends greatly on the initial distribution of surface species. As an example, we will focus on the complete decomposition of ammonia to produce $(Si)_3N$ structures (either B4-B4 or S4-S4; values shown in Table II). In the alternate distribution, structure S4-S4 is predicted to be more stable than structure A1-A1, while structure B4-B4 is less stable than A1-A1, suggesting that subsurface migration is more favorable thermodynamically. On the other hand, in the case of an aligned distribution, both B4 and S4 feature a lower stability than structure A1, suggesting that in this case total decomposition is not favored thermodynamically. Thus, the occurrence of a determined insertion pathway (and therefore the presence of certain surface structures) seems to be primarily determined by the initial distribution of surface species. It also suggests that one distribution may undergo insertion more easily than the other.

2. Orientation of inserted species

The effect of strain on the insertion processes can be enhanced or mitigated depending on the orientation of species on neighboring dimers, as shown in Table VI for the formation of the backbonded structure $(Si)_2NH$ (S2 or S2-S2, depending on the model employed). In addition, Table II shows that inward-outward orientations for structures B4-B4 and S2-S2 produce the least stable arrangement of the inserting structures because in this case the strain imposed by two neighboring structures has the same direction. When insertion is done in opposite directions, straining effects on one dimer are partially neutralized by the same effects on the neighboring dimer. The kinetics of insertion has been found to depend not only on the orientation of inserted structures but also on the saturation of the surface since mechanisms of strain relief are available providing that an inserted structure in the neighboring atom counteracts the strain effects during insertion.

3. Progress of an insertion reaction along the surface

Together with the influence of the initial distribution of adsorbates and their orientation during insertion, the feasibility of the process depends on the manner insertion takes place on the surface. We have analyzed a model where insertion of one adsorbate is completed before the neighboring adsorbate undergoes the same process (sequential model). Insertion processes have also been modeled assuming that a step-by-step, coordinated transformation of neighboring units occurs on the surface. However, this latter model does not seem to be as favorable as the sequential model because insertion mechanisms are less favorable when the neighboring structure features a tetracoordinated N atom (Tables IV and V), which was explained by the major displacement of Si atoms in the lattice when bonded to a tetracoordinated N atom. Thus, insertion processes on the surface are expected to be sequential, with one adsorbate finding a less demanding pathway if the neighboring dimers have already undergone the same transformation.

C. Brief evaluation of further theoretical approaches describing insertion processes on silicon surfaces

The use of a double-dimer cluster model has been shown to present significant advantages with respect to single-dimer models and its results have been observed to be in general agreement with the ones obtained using larger clusters (Sec. III D). However, it is important to re-emphasize that the appropriate simulation of a surface structure and insertion processes using this approach requires the absence of extreme rearrangements of atoms representing the immediate surroundings of the reaction. For cluster models to be employed in investigations of subsurface-insertion processes, the specifics of the insertion process have to be examined to avoid the problems with estimation of straining effects. For example, in Sec. III D, two different clusters were employed to

evaluate the effect of cluster size on the stability of the surface species. On the other hand, the use of slab models may constitute an interesting alternative for investigating the origin and mitigation of surface strain during insertion processes. However, in this case, it is important to bear in mind that the replication of only one dimer for structures featuring lateral insertion (e.g., S2) using slab models may result in the recreation of what we have called the inward-outward configuration, which has been postulated here to be the least stable orientation for backbonded structures. Thus, the supercell that is replicated should consist of at least two dimers along the same row. Moreover even in this case, the symmetry limitations may preclude one from evaluating multiple possible insertion pathways considered in this work based on simplified cluster models. Finally, although the possibility of inter-row straining effects has been neglected in this investigation, it may also play an important role that would be worth exploring in the future.

D. Implications for the control of adsorbate incorporation onto a surface

Adsorption on ordered surfaces has received increasing attention due to the desire for modifying and controlling the properties of a surface at the atomic and molecular levels. The computational results outlined above suggest that decomposition of these adsorbates may also take place through mechanisms that can lead to inserted species in self-oriented patterns along the surface. Thus, since the least energetically demanding arrangement of inserted structures is expected to prevail, specific patterns along the surface can be envisioned. The sequential nature of insertion processes indicate that they may occur as a "domino" reaction, where once a structure has been inserted (either naturally or promoted), the next structures along a dimer row can follow the transformation in an easier manner.

Our results also suggest that the occurrence of an insertion process is determined by the initial distribution of adsorbates, where one distribution is more likely to dissipate strain more efficiently than others. With several investigations supporting a temperature-dependent distribution of $(Si)NH_2$ species along the Si(100)-2×1 surface,[40,55–57,66] it is apparent that the occurrence of insertion processes can be controlled based on the adsorption temperature.[54] In addition, the saturation of the surface has to be taken into account, since the self-promoted mechanisms of insertion described here depend on the presence of an inserting structure in the neighboring dimer that eases the insertion process. At low coverages, cooperative insertion between neighboring dimers may not be possible, although it is likely that surface-insertion mechanisms prevail, due to the availability of reactive Si atoms on the surface.[43]

The control of the initial distribution of adsorbates on the surface, together with the self-controlled orientation of inserted species, would result in an unusual approach to surface functionalization, where not only the adsorption of functionalities can be controlled, but also the thermal transformation of the adsorbed species. Ultimately, the controlled insertion can lead to the formation of decomposed structures on the surface with different properties to those of the adsorbed species. Further investigations are needed in order to explore the possibilities outlined here.

V. CONCLUSIONS

The effect of surface strain on insertion processes has been investigated computationally taking the ammonia-covered Si(100)-2×1 surface as a model system. By using single- and double-dimer cluster models, it has been possible to observe the effects of strain on the site undergoing the insertion and on the neighboring surface sites, and an estimation of the stability loss due to straining effects on the surface can be obtained. Depending on how the strain affects the neighboring adsorption or reaction sites, insertion processes can be considered local or long ranging. Surface insertion into the Si-Si dimer bond has been observed to be rather local, and the presence of neighboring structures produces only a slight change in the energetics of insertion. On the other hand, subsurface insertion into the Si-Si backbond was found to have a long-ranging character, where the initial distribution of adsorbates and the orientation of inserted structures influence the occurrence of the insertion process, for they can enhance or hamper the straining effects on the surface.

Both insertion processes seem to be more favored if they take place in a sequential manner, with an adsorbate undergoing insertion once the neighboring site has already completed the same transformation. The orientation of insertion in this case is dictated by the neighboring inserted structure and would result in an arrangement that relieves (at least partially) the surface strain. Insertion in a coordinated manner is predicted to be less likely because the presence of structures bearing tetracoordinated N atoms turns the insertion into a more demanding process.

Application of these findings to the $NH_3/Si(100)$ system indicates that subsurface diffusion can be as favorable as surface insertion, in agreement with experimental observations. The possibility of a controlled pattern of inserted structures along the surface may open new opportunities for surface functionalization and other fields where surfaces are to be modified at the molecular level.

ACKNOWLEDGMENTS

This work was supported by the National Science Foundation (Grants No. CHE-0313803 and No. CHE-0650123). The National Science Foundation is also acknowledged for supporting this work through TeraGrid resources[67] provided by the National Center for Supercomputing Applications (NCSA) under Grant No. CHE070079N. GridChem (http://www.gridchem.org)[68,69] is acknowledged for computational resources and services for selected results used in this publication. D. J. Doren and Na Guo (Department of Chemistry and Biochemistry, University of Delaware) are acknowledged for their help with the computations using the $Si_{27}H_{24}$ and $Si_{32}H_{28}$ cluster models. J.C.F.R.-R. acknowledges the support of the University of Delaware through the Graduate Fellowship.

*Corresponding author. andrewt@udel.edu

[1] R. Q. Zhang, Y. L. Zhao, and B. K. Teo, Phys. Rev. B **69**, 125319 (2004).
[2] A. Agrawal, R. E. Butera, and J. H. Weaver, Phys. Rev. Lett. **98**, 136104 (2007).
[3] D. L. S. Nieskens, D. Curulla-Ferre, and J. W. Niemantsverdriet, ChemPhysChem **7**, 1022 (2006).
[4] F. Buatier de Mongeot, A. Cupolillo, M. Rocca, and U. Valbusa, Chem. Phys. Lett. **302**, 302 (1999).
[5] Y. Xia and R. Mokaya, Angew. Chem., Int. Ed. **42**, 2639 (2003).
[6] J. C. F. Rodríguez-Reyes and A. V. Teplyakov, Chem.-Eur. J. **13**, 9164 (2007).
[7] Z. Ma and F. Zaera, Surf. Sci. Rep. **61**, 229 (2006).
[8] M. A. Filler and S. F. Bent, Prog. Surf. Sci. **73**, 1 (2003).
[9] T. Leftwich and A. V. Teplyakov, Surf. Sci. Rep. **63**, 1 (2008).
[10] S. F. Bent, Surf. Sci. **500**, 879 (2002).
[11] K. Raghavachari and M. D. Halls, Mol. Phys. **102**, 381 (2004).
[12] C. H. Choi and M. S. Gordon, in *Computational Materials Chemistry: Methods and Application*, edited by L. A. Curtis and M. S. Gordon (Kluwer, The Netherlands, 2004), p. 125.
[13] J. A. Steckel and K. D. Jordan, in *Computational Materials Chemistry: Methods and Applications*, edited by L. A. Curtis and M. S. Gordon (Kluwer, The Netherlands, 2004), p. 246.
[14] G. P. Srivastava, Comput. Phys. Commun. **137**, 143 (2001).
[15] J. Yoshinobu, Prog. Surf. Sci. **77**, 37 (2004).
[16] M. J. Dresser, P. A. Taylor, R. M. Wallace, W. J. Choyke, and J. J. T. Yates, Surf. Sci. **218**, 75 (1989).
[17] M. Fujisawa, Y. Taguchi, Y. Kuwahara, M. Onchi, and M. Nishijima, Phys. Rev. B **39**, 12918 (1989).
[18] J. L. Bischoff, F. Lutz, D. Bolmont, and L. Kubler, Surf. Sci. **251-252**, 170 (1991).
[19] C. U. S. Larsson and A. S. Flodstrom, Surf. Sci. **241**, 353 (1991).
[20] E. Fattal, M. R. Radeke, G. Reynolds, and E. A. Carter, J. Phys. Chem. B **101**, 8658 (1997).
[21] N. Franco, J. Avila, M. E. Davila, M. C. Asensio, D. P. Woodruff, O. Schaff, V. Fernandez, K. M. Schindler, V. Fritzsche, and A. M. Bradshaw, Phys. Rev. Lett. **79**, 673 (1997).
[22] S. H. Lee and M. H. Kang, Phys. Rev. B **58**, 4903 (1998).
[23] R. Miotto, G. P. Srivastava, and A. C. Ferraz, Phys. Rev. B **58**, 7944 (1998).
[24] Z. Loh and H. C. Kang, J. Chem. Phys. **112**, 2444 (2000).
[25] K. T. Queeney, Y. J. Chabal, and K. Raghavachari, Phys. Rev. Lett. **86**, 1046 (2001).
[26] J.-Y. Lee and J.-H. Cho, J. Phys. Chem. B **110**, 18455 (2006).
[27] A. B. Gurevich, B. B. Stefanov, M. K. Weldon, Y. J. Chabal, and K. Raghavachari, Phys. Rev. B **58**, R13434 (1998).
[28] M. K. Weldon, B. B. Stefanov, K. Raghavachari, and Y. J. Chabal, Phys. Rev. Lett. **79**, 2851 (1997).
[29] B. B. Stefanov and K. Raghavachari, Surf. Sci. **389**, L1159 (1997).
[30] R. Konecny and D. J. Doren, J. Chem. Phys. **106**, 2426 (1997).
[31] Z. K. Smedarchina and M. Z. Zgierski, Int. J. Mol. Sci. **4**, 445 (2003).
[32] J. W. Kim, H. W. Yeom, K. J. Kong, B. D. Yu, D. Y. Ahn, Y. D. Chung, C. N. Whang, H. Yi, Y. H. Ha, and D. W. Moon, Phys. Rev. Lett. **90**, 106101 (2003).
[33] J. W. Kim and H. W. Yeom, Surf. Sci. **546**, L820 (2003).
[34] A. L. Gerrard, J. Chen, and J. F. Weaver, J. Phys. Chem. B **109**, 8017 (2005).
[35] X. Wang and X. Xu, J. Phys. Chem. C **111**, 16974 (2007).
[36] I. K. Cho, Y. K. Kim, and H. W. Yeom, Phys. Rev. B **73**, 115328 (2006).
[37] A. Hemeryck, N. Richard, A. Esteve, and M. Djafari Rouhani, Surf. Sci. **601**, 2339 (2007).
[38] B. R. Trenhaile, A. Agrawal, and J. H. Weaver, Appl. Phys. Lett. **89**, 151917 (2006).
[39] R. J. Eyre, J. P. Goss, and P. R. Briddon, Phys. Rev. B **76**, 245325 (2007).
[40] J. C. F. Rodríguez-Reyes and A. V. Teplyakov, Phys. Rev. B **76**, 075348 (2007).
[41] H.-J. Kim and J.-H. Cho, Phys. Rev. B **69**, 233402 (2004).
[42] X. Xu, S. Y. Kang, and T. Yamabe, Phys. Rev. Lett. **88**, 076106 (2002).
[43] Y. Widjaja and C. B. Musgrave, Phys. Rev. B **64**, 205303 (2001).
[44] T. L. McDonell, N. A. Marks, O. Warschkow, H. F. Wilson, P. V. Smith, and M. W. Radny, Phys. Rev. B **72**, 193307 (2005).
[45] P. Avouris, F. Bozso, and R. J. Hamers, J. Vac. Sci. Technol. B **5**, 1387 (1987).
[46] C. Bater, M. Sanders, and J. J. H. Craig, Surf. Interface Anal. **29**, 208 (2000).
[47] Y. Widjaja and C. B. Musgrave, Surf. Sci. **469**, 9 (2000).
[48] L. P. Méndez de Leo and A. V. Teplyakov, J. Phys. Chem. B **110**, 6899 (2006).
[49] D. B. Skliar, C. Gelmi, T. Ogunnaike, and B. G. Willis, Surf. Sci. **601**, 2887 (2007).
[50] K. A. Perrine, D. B. Skliar, B. G. Willis, and A. V. Teplyakov, Surf. Sci. **602**, 2222 (2008).
[51] J.-H. Cho and K. S. Kim, Phys. Rev. B **62**, 1607 (2000).
[52] M. Z. Zgierski and Z. K. Smedarchina, Europhys. Lett. **63**, 556 (2003).
[53] Y. Widjaja and C. B. Musgrave, J. Chem. Phys. **120**, 1555 (2004).
[54] Y. Wang and G. S. Hwang, J. Chem. Phys. **122**, 164706 (2005).
[55] O. N. Chung, H. Kim, S. Chung, and J.-Y. Koo, Phys. Rev. B **73**, 033303 (2006).
[56] O. N. Chung, H. Kim, J.-Y. Koo, and S. Chung, Phys. Rev. B **74**, 193312 (2006).
[57] D. R. Bowler and J. H. G. Owen, Phys. Rev. B **75**, 155310 (2007).
[58] O. Warschkow, T. L. McDonell, and N. A. Marks, Surf. Sci. **601**, 3020 (2007).
[59] A. D. Becke, J. Chem. Phys. **98**, 5648 (1993).
[60] C. Lee, W. Yang, and R. G. Parr, Phys. Rev. B **37**, 785 (1988).
[61] B. B. Stefanov and K. Raghavachari, Appl. Phys. Lett. **73**, 824 (1998).
[62] Y. Widjaja, M. M. Mysinger, and C. B. Musgrave, J. Phys. Chem. B **104**, 2527 (2000).
[63] C. Peng and H. B. Schlegel, Isr. J. Chem. **33**, 449 (1993).
[64] J. M. Frisch *et al.*, GAUSSIAN03, Revision C.02, Gaussian, Inc., Wallingford, CT, 2004.
[65] M. Z. Hossain, Y. Yamashita, K. Mukai, and J. Yoshinobu, Phys. Rev. B **68**, 235322 (2003).
[66] J. H. G. Owen, D. R. Bowler, S. Kusano, and K. Miki, Phys. Rev. B **72**, 113304 (2005).

[67] C. Catlett *et al.*, in *Advances in Parallel Computing*, edited by L. Grandinetti (IOS, Amsterdam, 2007), Vol. 16, p. 225.

[68] R. Dooley, K. Milfeld, K. Guiang, S. Pamidighantam, and G. Allen, J. Grid. Comput. **4**, 195 (2006).

[69] K. Milfeld, C. Guiang, S. Pamidighantam, and J. Giuliani, Proceedings of the Sixth LCI International Conference on Linux Clusters: The HPC Revolution, North Carolina, 2005 (unpublished).